

## 謝誌

碩士班兩年的研究生涯，踏入了一個全新的領域，一切得從基礎開始學起，說實在這兩年來歷經的壓力和挫折真的不少，但多虧了一路上許多人的支持幫助與鼓勵，才能讓我順利完成論文，同時獲得了無價的成長；首先，最感謝的就是我的指導教授 張淑閔老師，張老師除了很有耐心地將我們從最基本帶起，在價值觀及做人處事的態度上也給了我很大的影響及啟發，讓我知道做研究正確的態度及精神，也體會到「求知」原來是一件具挑戰性又快樂的事情，更重要的是學習時間管理、情緒控制和自我要求，兩年下來，真的改變我很多。也很感謝董瑞安老師無論是在實驗設備或是論文研究上給予我們幫助及指導，同時感謝白曠綾老師、黃暄益老師及閻明宇博士對於我論文撰寫及研究方向的建議和指導，使我的論文能更趨於充實完善。

另外，要感謝跟我一樣同是實驗室第一屆唯二研究生的侯傑耀，我們一起歷經建立實驗室的辛苦和調整心態的壓力，理性又努力的他總是適時地給我幫助和鼓勵，是我研究路上少數的依靠，學妹品涵、維斯和學弟精榮的加入讓實驗室變得更熱鬧，也讓日常生活少了寂寞而更添歡樂。謝謝董老師實驗室的學長添進、俊錡、平善、學姐世芬、世慧、家敏以及同學涵云、依琳、唐興在實驗上給予我的幫助，很多事情都願意不厭其煩地協

助我或幫我解答，在你們身上我學到不少做研究和處理事情的態度。謝謝同是大學和研究所同學，並身兼五年室友的好友孝綸和琪婷，有妳們，讓我這兩年不孤單；謝謝學長智淵，這兩年如果沒有你的陪伴和鼓勵，很多挫折和瓶頸都很難獨自面對，更感謝你在生活上給予我的照顧，讓我能無後顧之憂地面對眼前的壓力。另外，感謝椰伶成康的大家，無論我身在何處，你們永遠是我心裡的避風港。

最後要感謝我的家人，一直鼓勵我唸書，提供我不虞匱乏的物質生活，總是關心和原諒我錯誤的爸媽，還有像朋友一樣，願意聽我所有心事和抱怨的弟弟，沒有你們，這條路走不下去，也真的很謝謝你們的支持，這篇論文獻給你們，謝謝你們相信我，體諒我，讓我能完成論文，同時向下個階段挑戰。

品欣

九十六年八月三十

## 中文摘要

本研究內容主要為利用自行合成之聚苯乙烯 (polystyrene) 為模版，配合溶膠-凝膠法製備多孔性的二氧化鈦以及二氧化矽材料，再以表面溶膠-凝膠將二氧化鈦光觸媒鍍於多孔二氧化矽材料的表面，使光觸媒以超薄膜之型態穩固地附著於基材表面，製備出骨-膚 (bone-skin) 型態的多孔複合光觸媒材料。

在此研究中，聚苯乙烯經由乳化聚合法合成，並以十二烷基磺酸鈉(Sodium dodecyl sulfate, SDS) 作為穩定劑，其最佳條件為加入1 CMC 之SDS，反應溫度為80 °C，經預熱過程合成出之單一分散性聚苯乙烯小球 (直徑約190 nm)。在此條件下合成出之聚苯乙烯小球，經重力沈降排列後作為模版，再將二氧化矽前驅物填充入模版間隙內，經溶膠-凝膠反應後，利用鍛燒將模版移除以獲得具規則孔洞排列之多孔性二氧化矽基材。之後利用表面溶膠-凝膠將二氧化鈦以超薄膜之型態鍍於多孔二氧化矽材料的表面，製備出骨-膚多孔複合光觸媒材料。同時會進行自行製備之光觸媒其表面物化特性之鑑定，並藉由其與單純多孔性二氧化鈦光觸媒光降解 Rhodamine B 染劑之效果，比較兩者之光催化能力。

結果顯示自行製備之骨-膚多孔複合光觸媒材料不僅維持量子特性且具有高比表面積 (410.5 ~ 534.9 m<sup>2</sup>/g)，對於Rh B 染劑之降解也具有高比光催化活性 ( $2.9 \times 10^{-2} \sim 3.6 \times 10^{-2} \text{ min}^{-1}\text{mg}^{-1}$ )。由溶膠-凝膠法製備而成之二氧化鈦超薄膜，其膜厚 (4.6 ~ 9.4 nm) 可藉由在表面溶膠-凝膠之過程中，調控二氧化鈦前驅物之濃度，以達到良好的控制；骨-膚多孔複合光觸媒之光活性亦和二氧化鈦超薄膜之厚度有高度的相關性。在二氧化鈦前驅物和異丙醇之重量比為 0.2 之條件下製備而成的骨-膚多孔二氧化矽-二氧化鈦複合光觸媒具有最高的比光催化活性，此結果可歸因於其大比表面積以及二氧化鈦超薄膜所提供之較短電荷擴散路徑。同時，在此研究中，也將會探討光觸媒物化特性對其光催化活性的影響以及兩者之間的關係。

## Abstract

In this study, the ultra-thin TiO<sub>2</sub> films were coated onto the highly porous silica to form bone-skin-like photocatalysts with controllable film thickness and high photoactivity by the combination of templating sol-gel method and surface sol-gel method. Monodisperse polystyrene microspheres in this study were prepared by emulsion polymerization method with sodium dodecyl sulfate (SDS) as stabilizer. The optimal condition to synthesize monodisperse polystyrene is reacting at 80 °C in a preheated procedure when 1 CMC of SDS was added. The resulting monodisperse polystyrene microspheres with a diameter of about 190 nm were used as templates to fabricate the porous framework by infilling sol-gel derived silica into the voids between microspheres. The porous silica framework (bone structure) with ordered hexagonal porous structures in three dimensions was obtained by subsequently removing microspheres with calcinations. The ultra-thin TiO<sub>2</sub> layers obtained from the surface sol-gel method were then coated on the surface of the porous silica framework to form the bone-skin-like structures. Results showed that the developed bone-skin-like porous photocatalyst has a high surface area (410.5 ~ 534.9 m<sup>2</sup>/g) and retains quantum properties to perform the novelty on high specific photocatalytic activities ( $2.9 \times 10^{-2} \sim 3.6 \times 10^{-2} \text{ min}^{-1} \text{ mg}^{-1}$ ). The thickness of the sol-gel-derived TiO<sub>2</sub> thin films ranged from 4.6 to 9.4 nm can be well-controlled by simply adjusting the concentrations of the TiO<sub>2</sub> precursors in the surface sol-gel process, while the photoactivity of the photocatalysts is highly dependent on the thicknesses of the ultra-thin TiO<sub>2</sub> coatings. The bone-skin-like SiO<sub>2</sub>/TiO<sub>2</sub> with the precursor concentration of 0.2 had the highest specific photocatalytic activity due to the highest surface area and short charge diffusion length. The relationship between degradation rate and physicochemical properties of photocatalysts was also discussed in this study.

## Content Index

謝誌.....	i
中文摘要.....	iii
Abstract.....	iv
Content Index.....	v
Table Index.....	vii
Figure Index.....	viii

## Content Index

CHAPTER 1. INTRODUCTION.....	1
1.1 Motivation.....	1
1.2 Objective.....	4
CHAPTER 2. LITERATURE REVIEW.....	5
2.1 Photocatalysis.....	5
2.1.1 Principle of photocatalysis.....	5
2.1.2 Photocatalyst.....	9
2.2 Colloidal crystal templating metho.....	12
2.3 Principle of Emulsion Polymerization.....	17
2.4 Sol-gel method.....	21
2.5 Surface Sol-gel method.....	24
CHAPTER 3. MATERIALS AND METHODS.....	26
3.1 Chemicals.....	26
3.2 Synthesis of polystyrene microspheres.....	28
3.3 Fabrication of porous titania and silica.....	30
3.4 Preparation of bone-skin-like photocatalysts.....	32
3.5 Photodegradation of Rhodamine B.....	33
3.6 Characterization.....	35

CHAPTER 4. RESULTS AND DISCUSSION .....	36
4.1 Preparation of Polystyrene Microspheres .....	36
4.1.1 Effects of heating procedure and surfactant concentration .....	36
4.1.2 Effects of reaction temperature .....	38
4.2 Morphology of Porous TiO <sub>2</sub> and bone-skin-like SiO <sub>2</sub> /TiO <sub>2</sub> .....	40
4.3 Texture of Porous TiO <sub>2</sub> and bone-skin-like SiO <sub>2</sub> /TiO <sub>2</sub> .....	46
4.4 Crystalline properties of Porous TiO <sub>2</sub> and bone-skin-like SiO <sub>2</sub> /TiO <sub>2</sub> .....	51
4.5 Optical properties of Porous TiO <sub>2</sub> and bone-skin-like SiO <sub>2</sub> /TiO <sub>2</sub> .....	56
4.6 EPR studies of Porous TiO <sub>2</sub> and bone-skin-like SiO <sub>2</sub> /TiO <sub>2</sub> .....	60
4.7 Photoactivities- Degradation of Rhodamine B .....	65
CHAPTER 5. CONCLUSIONS .....	72
Literature Cited .....	73
Appendix A. Operation parameters of the instruments .....	75
Appendix B. Nitrogen adsorption-desorption isotherms .....	78

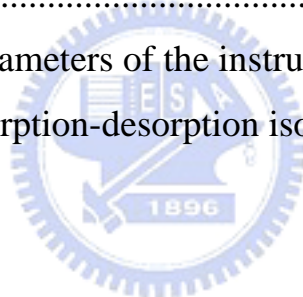


## Table Index

Table 2-1	Fabrication of porous materials by colloidal crystal templating. ....	16
Table 3-1	The structures of chemicals used in this study.....	27
Table 4-1	Structural properties of various porous photocatalysts.....	44
Table 4-2	Pore-wall properties of porous TiO <sub>2</sub> and bone-skin-like SiO <sub>2</sub> /TiO <sub>2</sub> with various weight ratios of alkoxide/solvent. ....	50
Table 4-3	Crystalline sizes porous TiO <sub>2</sub> and SiO <sub>2</sub> /TiO <sub>2</sub> with various weight ratios of alkoxide/solvent.....	53
Table 4-4	The bandgap energies of all porous samples. ....	59
Table 4-5	Summary of EPR parameters and the assignments of the signals obtained in this study.....	63
Table 4-6	The intensities of all signals obtained from the integrations of the spectra.....	64
Table 4-7	The weight percentages of silica and titania and the real contents of TiO <sub>2</sub> in bone-skin-like porous photocatalysts with different precursor concentrations. ..	68
Table 4-8	The photocatalytic activities of various porous photocatalysts .....	71

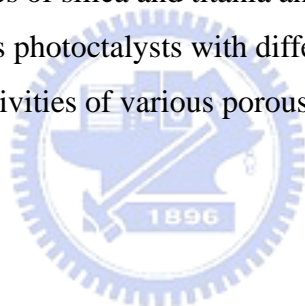


## Figure Index

Figure 2-1	Reaction diagram of photocatalysis at a semiconductor by illumination... ..5	5
Figure 2-2	Schematic photoexcitation in a solid followed by deexcitation events.....6	6
Figure 2-3	The band edge derived from the flat band potentials positions of several semiconductors in a contact solution of aqueous electrolyte at pH = 1.....10	10
Figure 2-4	Structure of rutile and anatase TiO <sub>2</sub> .....11	11
Figure 2-5	Positions of the redox potentials of various metallic couples related to the energy levels of the conduction and valence bands of TiO <sub>2</sub> Degussa P-25 at pH=0.....12	12
Figure 2-6	Schematic of the general procedure for replicating the structure of colloidal crystals into porous materials.....14	14
Figure 2-7	The two possible modes of propagation: (I) head-to-tail addition (II) head-to-head addition.....19	19
Figure 2-8	Schematic diagram illustrating the process of emulsion polymerisation.....21	21
Figure 2-9	The sol-gel technologies and the various forms of products.....22	22
Figure 2-10	The reaction mechanism of sol-gel process.....23	23
Figure 2-11	The four steps included in surface sol-gel process.....25	25
Figure 3-1	The experimental device of emulsion polymerization.....29	29
Figure 3-2	The mechanism of oil-in-water emulsion polymerization of polystyrene... ..29	29
Figure 3-3	The preparation of the latex arrangements by deposition on filtration membranes.....31	31
Figure 3-4	Schematic diagram illustrating the addition of precursor solution to the template.....31	31
Figure 3-5	The experimental device of the preparation of bone-skin-like photocatalysts.....33	33
Figure 3-6	The instrument of photoreactor.....34	34
Figure 4-1	SEM images of polystyrene synthesized at various conditions.....39	39
Figure 4-2	TEM and SEM micrographs of porous TiO <sub>2</sub> with different weight ratios of metal alkoxide/solvent.....41	41
Figure 4-3	TEM images of porous SiO <sub>2</sub> (A) and bone-skin-like porous SiO <sub>2</sub> /TiO <sub>2</sub> with weight ratios of alkoxide/solvent of 0.2 (B), 0.6 (C) and 1.2 (D). Insert in (A) shows the SEM image of porous SiO <sub>2</sub> .....43	43



Figure 4-4	TEM images of bone-skin-like porous SiO <sub>2</sub> /P25 with different concentration.....	45
Figure 4-5	Nitrogen adsorption-desorption isotherm of porous TiO <sub>2</sub> with the precursor concentration of 0.6.....	48
Figure 4-6	Nitrogen adsorption-desorption isotherms (inset) and corresponding BJH pore-size distribution curves of porous SiO <sub>2</sub> /TiO <sub>2</sub> with precursor concentration of 0.6.....	48
Figure 4-7	Nitrogen adsorption-desorption isotherm of porous SiO <sub>2</sub> /P-25 with the TiO <sub>2</sub> concentration of 0.6.....	49
Figure 4-8	XRD patterns of porous TiO <sub>2</sub> with various weight ratios of metal alkoxide/solvent.....	52
Figure 4-9	XRD patterns of bone-skin-like porous SiO <sub>2</sub> /TiO <sub>2</sub> with various weight ratios of TTIP/solvent and porous SiO <sub>2</sub> .....	52
Figure 4-10	XRD patterns of bone-skin-like porous SiO <sub>2</sub> /P-25 with various slurry concentrations.....	53
Figure 4-11	HRTEM images of bone-skin-like porous SiO <sub>2</sub> /TiO <sub>2</sub> with precursor concentrations of 0.2 (A), 0.6 (B) and 1.2 (C) and porous SiO <sub>2</sub> /P-25 with TiO <sub>2</sub> concentration of 0.6 (D,E).....	55
Figure 4-12	UV-Vis spectra shows the optical properties of the porous TiO <sub>2</sub> with different metal alkoxide/solvent weight ratios.....	57
Figure 4-13	UV-Vis spectra shows the optical properties of the porous SiO <sub>2</sub> /TiO <sub>2</sub> with different metal alkoxide/solvent weight ratios.....	57
Figure 4-14	UV-Vis spectra shows the optical properties of the porous SiO <sub>2</sub> /P-25 with various slurry concentrations.....	58
Figure 4-15	EPR spectra of porous TiO <sub>2</sub> with various precursor concentrations measured at 77 K under UV irradiation.....	62
Figure 4-16	EPR spectra of porous SiO <sub>2</sub> /TiO <sub>2</sub> with various precursor concentrations measured at 77 K under UV irradiation.....	62
Figure 4-17	EPR spectra of porous SiO <sub>2</sub> /P-25 with various TiO <sub>2</sub> concentrations measured at 77 K under UV irradiation.....	63
Figure 4-18	The photocatalytic activities of porous TiO <sub>2</sub> with various weight ratios of alkoxide/solvent.....	69
Figure 4-19	The photocatalytic activities of porous SiO <sub>2</sub> /TiO <sub>2</sub> with various weight ratios of alkoxide/solvent.....	69

Figure 4-20 The photocatalytic activities of porous SiO<sub>2</sub>/P-25 with various weight ratios of alkoxide/solvent.....70

